CHAPTER IV
RESULTS AND DISCUSSION

4.1 Analysis of Standard Chromatogram

The standard substances, which are *tert*-butanol, cyclohexene, cyclohexene oxide, 2-cyclohexen-1-ol, 2-cyclohexen-1-one, and (1S,2S)-*trans*-1,2-cyclohexanediol, were mixed with dodecane used the internal standard. The mixture was analyzed by a GC-FID in order to obtain the retention time of each substance. The chromatogram of the standard mixture is shown in Figure 4.1.

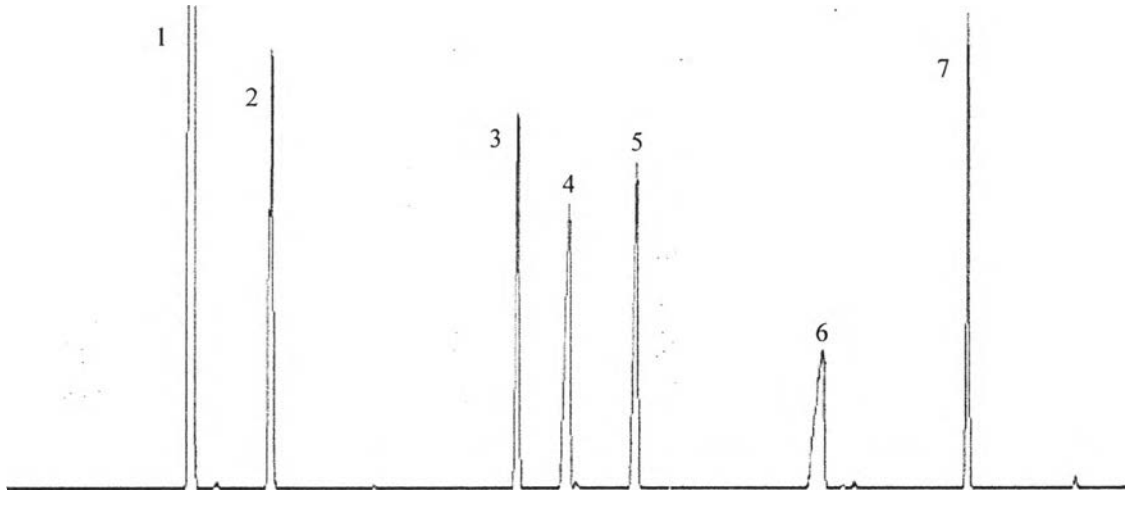

Figure 4.1 Chromatogram of the standard mixture: (1) *tert*-butanol, (2) cyclohexene, (3) cyclohexene oxide, (4) 2-cyclohexen-1-ol, (5) 2-cyclohexen-1-one, (6) (1S,2S)-*trans*-1,2-cyclohexanediol, and (7) dodecane.

The retention times of cyclohexene, cyclohexene oxide, 2-cyclohexen-1-ol, 2-cyclohexen-1-one, (1S,2S)-*trans*-1,2-cyclohexanediol, and dodecane are shown in Table 4.1.

Table 4.1 Retention time of each substance obtained from the chromatogram of the standard mixture

Number	Substance	Retention time (min)
1	*Tert*-butanol (solvent)	3.12
2	Cyclohexene	4.56
3	Cyclohexene oxide	8.78
4	2-Cyclohexen-1-ol	9.79
5	2-Cyclohexen-1-one	10.92
6	(1S,2S)-*trans*-1,2-cyclohexanediol	13.78
7	Dodecane	16.20

It can be seen from Table 4.1 that the retention time of dodecane internal standard was approximately at 16.20 min, which clearly separates from those of the reactant and possible products. It could be pointed out that dodecane is suitable to be used as the internal standard for this reaction. The response factor of each product was then calculated from the chromatogram of the standard mixture, and the results are shown in Table 4.2.

Table 4.2 Response factor of each substance obtained from the chromatogram of the standard mixture

Substance	Response factor
Cyclohexene	0.93
Cyclohexene oxide	0.80
2-Cyclohexen-1-ol	0.90
2-Cyclohexen-1-one	0.87
(1S,2S)-*trans*-1,2-cyclohexanediol	0.64
Dodecane	1.00

4.2 Catalyst Characterization Results

4.2.1 TG-DTA Results

The TG-DTA analysis was used to investigate the thermal decomposition behavior of the as-synthesized dried TiO_2-CeO_2 mixed oxide gels and to obtain their suitable calcination temperature. Figure 4.2 exemplifies the TG-DTA curves of the dried $0.95TiO_2$-$0.05CeO_2$ mixed oxide gel. The DTA curve shows three main exothermic regions. The first exothermic peak, with its position lower than 120 °C, could be ascribed to the removal of physisorbed water molecules. The second exothermic peak between 120 and 280 °C was attributed to the removal of the surfactant molecules (LACH) and modifying agent molecules (ACA). The third exothermic peak between 280 and 500 °C corresponded to the crystallization of catalyst and the elimination of organic remnants and chemisorbed water molecules. The TG curve shows that the weight loss ended at approximately 450 °C. Therefore, the results confirm that the calcination temperature equal to or higher than 450 °C was sufficient for the complete surfactant removal and the catalyst crystallization.

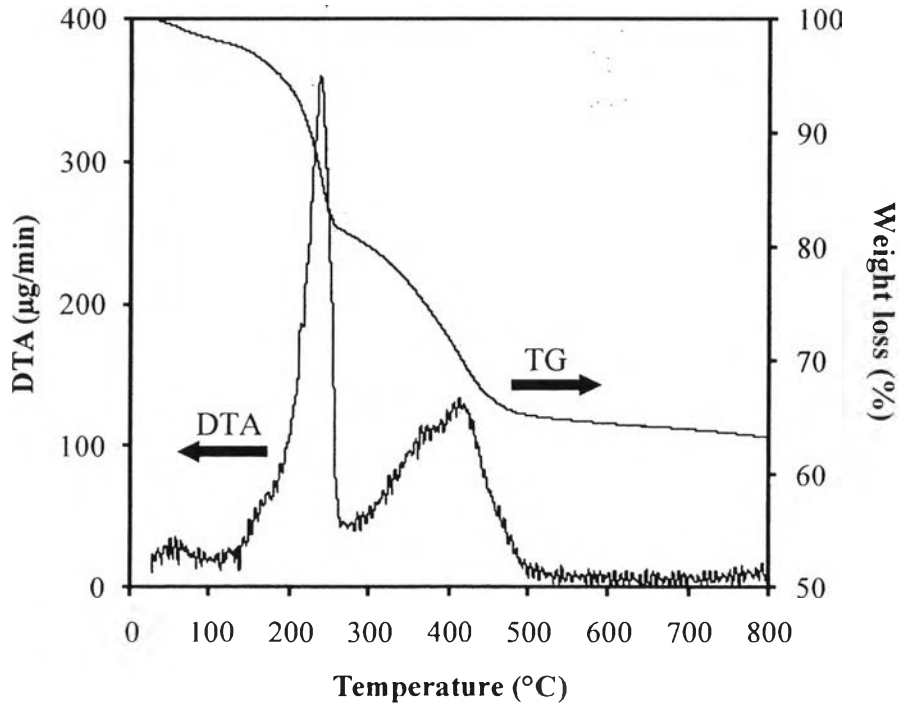

Figure 4.2 TG-DTA curves of the as-synthesized dried $0.95TiO_2$-$0.05CeO_2$ mixed oxide gel.

Moreover, the TG analysis was used to determine the surface OH density (OH/nm^2) and surface OH-to-catalyst weight ratio (OH/g). Figures 4.3 exemplifies the TG curve of the synthesized mesoporous-assembled $0.98TiO_2$-$0.02CeO_2$ mixed oxide catalyst calcined at 500 °C. The TG curve could be divided into two regions. The first region, with temperature lower than 120 °C, was attributable to the removal of physisorbed water molecules, as aforementioned, where this region is not crucial for powder characterization as it depends only on humidity from the environment. The second region, with temperature in the range of 120 to 500 °C, represented the weight loss by the removal of hydroxyl groups from the powder surface. The details of the surface OH density and surface OH-to-catalyst weight ratio of the synthesized mesoporous-assembled TiO_2-CeO_2 mixed oxide catalysts calcined at different temperatures are summarized in Tables 4.3. It can be seen from Table 4.3 that both the surface OH density and surface OH-to-catalyst weight ratio tended to increase with increasing CeO_2 content in the TiO_2-CeO_2 mixed oxide catalyst to reach maximum values at the CeO_2 content of 2 mol% (i.e. $0.98TiO_2$-$0.02CeO_2$), but they adversely decreased with further increasing CeO_2 content. These results indicate that the incorporation of CeO_2 with the suitable content to the TiO_2 could increase the number of surface OH groups available for the reaction. In the same manner, with increasing calcination temperature from 450 to 600 °C for the synthesized mesoporous-assembled $0.98TiO_2$-$0.02CeO_2$ mixed oxide catalyst, the maximum surface OH density and surface OH-to-catalyst weight ratio were observed at the calcination temperature of 500 °C. At a calcination temperature lower than 500 °C, the small quantity of organic remnants may still exist on the catalyst surface as OH group-binding species, whereas the OH groups may be thermally removed by severe calcination temperature higher than 500 °C. It can be suggested that a good control of calcination temperature could maintain a high level of surface OH groups.

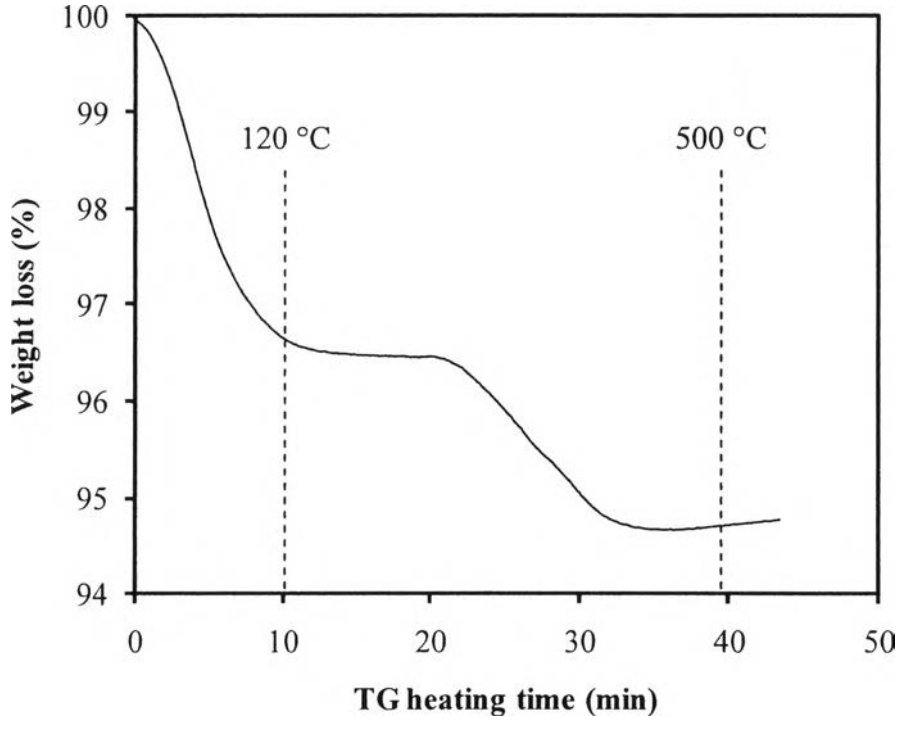

Figure 4.3 TG curve of the synthesized mesoporous-assembled $0.98TiO_2$-$0.02CeO_2$ mixed oxide catalyst calcined at 500 °C.

Table 4.3 Surface OH density and surface OH-to-catalyst weight ratio of the synthesized mesoporous-assembled TiO_2-CeO_2 mixed oxide catalysts calcined at different temperatures

Catalyst	Calcination temperature (°C)	$w_{120°C}$ (mg)	$w_{500°C}$ (mg)	OH/nm^2	OH/g ($\times 10^{-20}$)
Pure TiO_2	500	10.31	10.19	6.88	6.59
$0.99TiO_2$-$0.01CeO_2$		10.89	10.73	6.69	6.01
$0.98TiO_2$-$0.02CeO_2$		10.73	10.52	7.53	6.83
$0.97TiO_2$-$0.03CeO_2$		10.27	10.10	6.59	6.27
$0.95TiO_2$-$0.05CeO_2$		10.58	10.37	6.82	6.23
$0.93TiO_2$-$0.07CeO_2$		10.25	10.06	5.52	5.22
$0.90TiO_2$-$0.10CeO_2$		10.75	10.56	4.89	4.40
$0.98TiO_2$-$0.02CeO_2$	450	10.09	9.93	4.74	4.43
	500	10.73	10.52	7.53	6.83
	550	10.34	10.17	7.12	6.65
	600	10.60	10.48	5.26	4.86

4.2.2 N_2 Adsorption-Desorption Results

The N_2 adsorption-desorption analysis at the liquid N_2 temperature was used to the study mesoporosity and textural properties of the synthesized TiO_2-CeO_2 mixed oxide catalysts. The N_2 adsorption-desorption isotherms and pore size distribution (inset) of the synthesized mesoporous-assembled $0.98TiO_2$-$0.02CeO_2$ mixed oxide catalyst calcined at 500 °C are exemplified in Figure 4.4. It could be seen that the isotherms of the catalyst exhibited typical IUPAC type IV pattern with H2-type hysteresis loop, which is the main characteristic of mesoporous materials (mesoporous size between 2 and 50 nm) according to the classification of IUPAC (Rouquerol *et al.*, 1999). The shape of the isotherms reveals the structural characteristic of the catalyst powders, which was composed of an assembly of particles with narrow and uniform pore size, as clearly seen from the inset of Figure 4.4. The textural properties obtained from the isotherms and pore size distribution,

namely specific surface area, mean mesopore diameter, and total pore volume, of the synthesized mesoporous-assembled TiO_2-CeO_2 mixed oxide catalysts are given in Table 4.4. It could be observed that the incorporation of CeO_2 to the TiO_2 significantly increased the specific surface area and total pore volume of the TiO_2-CeO_2 mixed oxide catalysts (Pavasupree *et al.*, 2004), whereas the mean mesopore diameter only slightly changed. Interestingly, it was found that even though the specific surface area increased with increasing CeO_2 content, the surface OH density and surface OH-to-catalyst weight ratio progressively decreased when the CeO_2 content exceeded 2 mol% (Table 4.3). This is possibly because of the imperfect crystallization of the mesoporous-assembled TiO_2-CeO_2 mixed oxide catalysts at high CeO_2 contents, as shown next in section 4.2.3. The specific surface area, mean mesopore diameter, and total pore volume results of the synthesized mesoporous-assembled $0.98TiO_2$-$0.02CeO_2$ mixed oxide catalyst calcined at different temperatures are also shown in Table 4.4. The increase in calcination temperature resulted in the decrease in specific surface area and the increase in mean mesopore diameter, whereas the total pore volume only slightly decreased. The perceived loss in specific surface area can be explainable to the pore coalescence due to the crystallization of wall separating mesopores and the sintering of catalyst particles (Lin *et al.*, 2007), consequently resulting in the decrease in surface OH groups (Table 4.3).

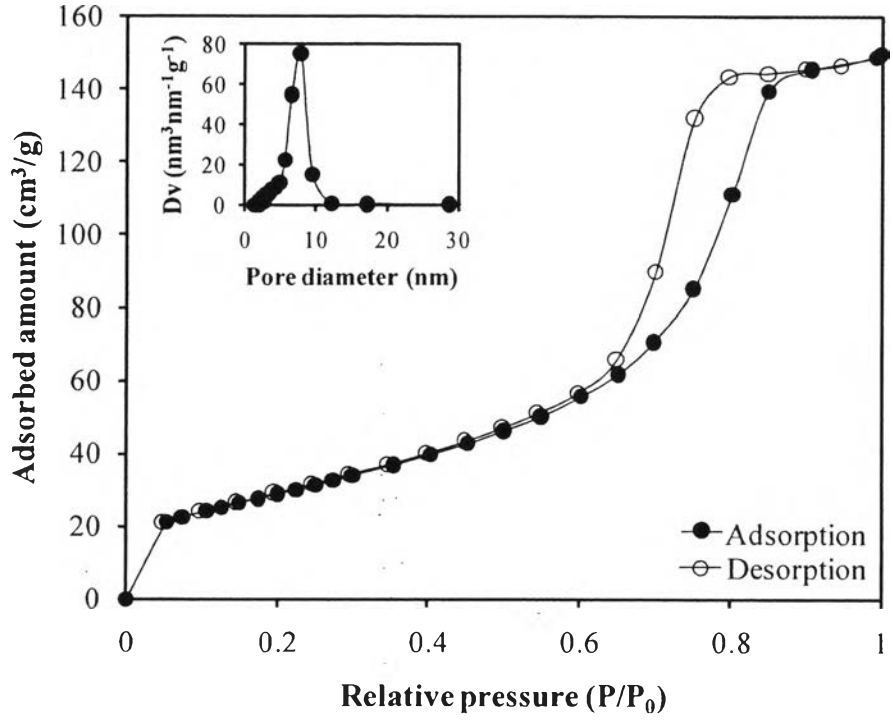

Figure 4.4 N_2 adsorption-desorption isotherms and pore size distribution (inset) of the synthesized mesoporous-assembled $0.98TiO_2$-$0.02CeO_2$ mixed oxide catalyst calcined at 500 °C.

Table 4.4 N_2 adsorption-desorption results of the synthesized mesoporous-assembled TiO_2-CeO_2 mixed oxide catalysts calcined at different temperatures

Catalyst	Calcination temperature (°C)	Specific surface area (m^2/g)	Mean mesopore diameter (nm)	Total pore volume (cm^3/g)
Pure TiO_2	500	63.4	8.10	0.12
$0.99TiO_2$-$0.01CeO_2$		91.9	9.14	0.21
$0.98TiO_2$-$0.02CeO_2$		107.0	7.83	0.24
$0.97TiO_2$-$0.03CeO_2$		105.0	7.80	0.26
$0.95TiO_2$-$0.05CeO_2$		121.6	6.54	0.23
$0.93TiO_2$-$0.07CeO_2$		136.2	10.06	0.34
$0.90TiO_2$-$0.10CeO_2$		153.8	8.75	0.34
$0.98TiO_2$-$0.02CeO_2$	450	144.6	4.90	0.24
	500	107.0	7.83	0.24
	550	101.6	6.59	0.22
	600	84.0	7.21	0.20

4.2.3 XRD Results

The XRD analysis was used to identify crystalline phases present in the synthesized catalysts. The XRD patterns of the synthesized mesoporous-assembled TiO_2-CeO_2 mixed oxide catalysts with different CeO_2 contents calcined at 500 °C are shown in Figure 4.5. The XRD patterns of all the investigated catalysts exhibited crystalline structure of the pure anatase TiO_2 phase owing to the observed dominant peaks at 2θ of about 25.6°, 38.0°, 48.2°, 53.8°, and 54.8°, which represent the indices of (101), (004), (200), (105), and (211) planes, respectively (Smith, 1960). However, the peak intensities decreased with increasing CeO_2 content possibly because a further increase in CeO_2 content retards the crystallization process of TiO_2 (Pavasupree *et al.*, 2004). The crystallite sizes of the mesoporous-assembled TiO_2-CeO_2 mixed oxide catalysts calculated using the Scherrer equation are shown in Table 4.5. It can be seen that the crystallite size decreased with increasing CeO_2 content due to the crystallization retardation, as mentioned above.

The XRD patterns of the synthesized mesoporous-assembled $0.98TiO_2$-$0.02CeO_2$ mixed oxide catalyst calcined at different temperatures are shown in Figure 4.6. The XRD patterns of the synthesized mesoporous-assembled $0.98TiO_2$-$0.02CeO_2$ catalyst also showed only crystalline structure of the pure anatase TiO_2 phase, and the anatase TiO_2 phase was maintained at the calcination temperature of as high as 600 °C without its partial transformation to the rutile TiO_2 phase normally observed at this high calcination temperature (Sreethawong *et al.*, 2005). As expected, the higher crystallite size of the anatase TiO_2 phase was observed at a higher calcination temperature (Table 4.5), possibly resulting in the decrease in the surface OH groups as well (Table 4.3).

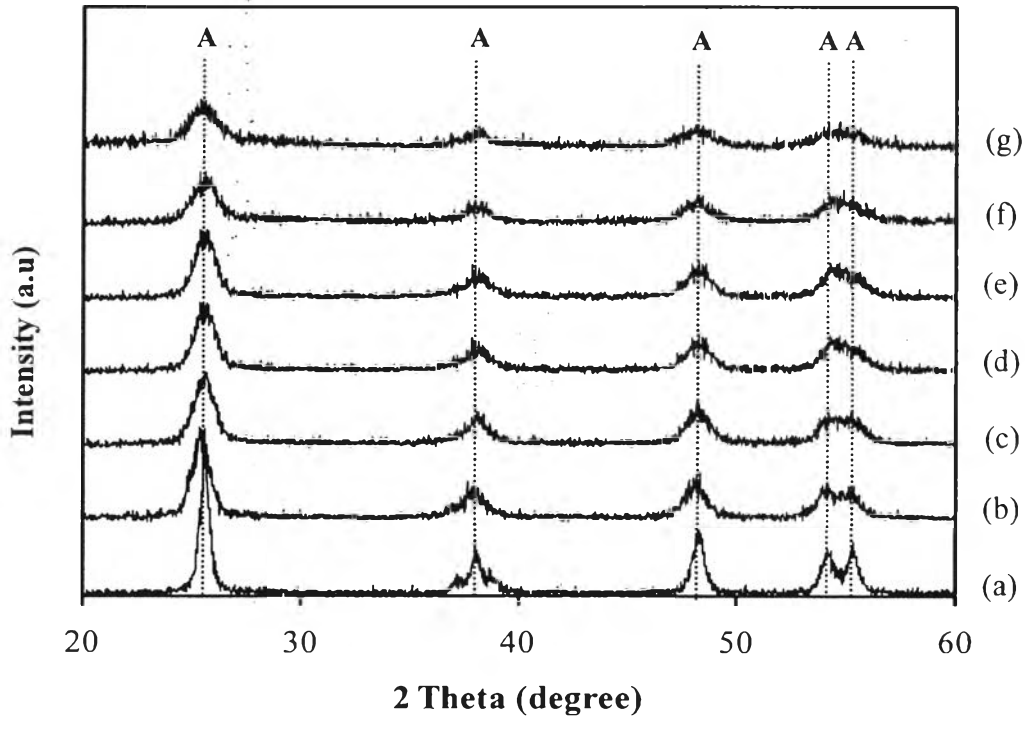

Figure 4.5 XRD patterns of the synthesized mesoporous-assembled TiO_2-CeO_2 mixed oxide catalysts calcined at 500 °C: (a) pure TiO_2, (b) $0.99TiO_2$-$0.01CeO_2$, (c) $0.98TiO_2$-$0.02CeO_2$, (d) $0.97TiO_2$-$0.03CeO_2$, (e) $0.95TiO_2$-$0.05CeO_2$, (f) $0.93TiO_2$-$0.07CeO_2$, and (g) $0.90TiO_2$-$0.10CeO_2$ (A: Anatase TiO_2).

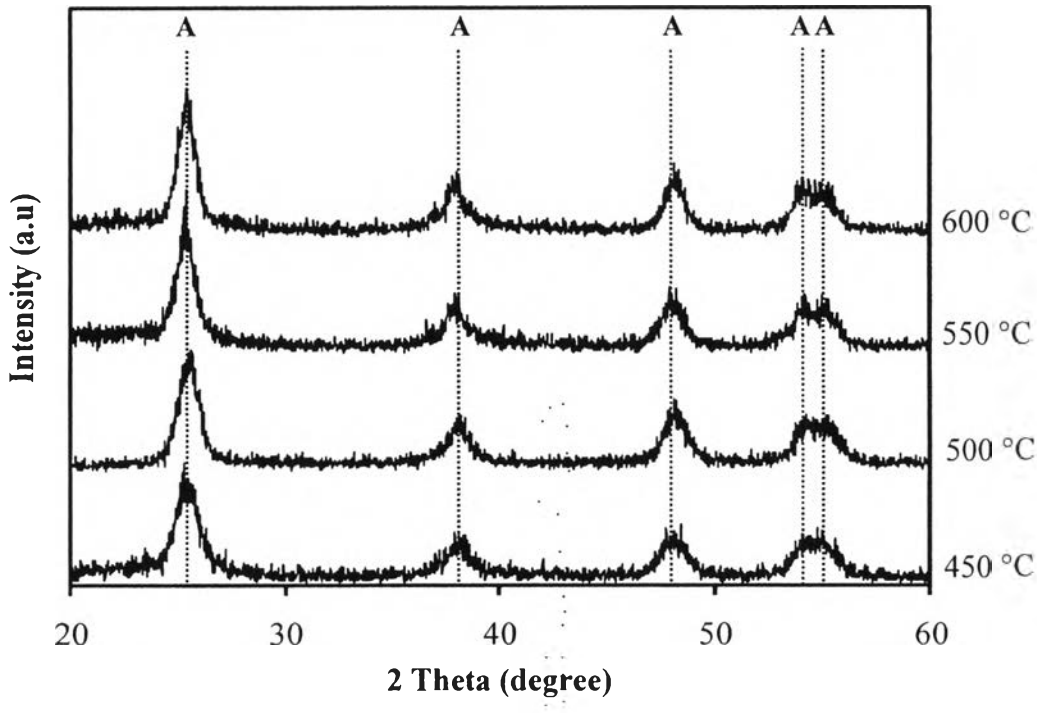

Figure 4.6 XRD patterns of the synthesized mesoporous-assembled $0.98TiO_2$-$0.02CeO_2$ mixed oxide catalysts calcined at different temperatures (A: Anatase TiO_2).

Table 4.5 Crystallize size results of the synthesized mesoporous-assembled TiO_2-CeO_2 mixed oxide catalysts calcined at different temperatures

Catalyst	Calcination temperature (°C)	Anatase (101) crystallite size (nm)
Pure TiO_2	500	15.62
$0.99TiO_2$-$0.01CeO_2$		9.04
$0.98TiO_2$-$0.02CeO_2$		6.93
$0.97TiO_2$-$0.03CeO_2$		6.94
$0.95TiO_2$-$0.05CeO_2$		6.23
$0.93TiO_2$-$0.07CeO_2$		5.76
$0.90TiO_2$-$0.10CeO_2$		5.49
$0.98TiO_2$-$0.02CeO_2$	450	6.38
	500	6.93
	550	8.09
	600	8.69

4.2.4 SEM-EDX and TEM-EDX Results

The information about the surface morphology and elemental distribution of the synthesized mesoporous-assembled TiO_2-CeO_2 mixed oxide catalysts was obtained by the SEM analysis. Figure 4.7 exemplifies the SEM image of the mesoporous-assembled $0.98TiO_2$-$0.02CeO_2$ mixed oxide catalyst calcined at 500 °C. The catalyst nanoparticles with quite uniform size could be observed in the form of aggregated clusters containing many nanoparticles. The elemental distributions on the mesoporous-assembled $0.98TiO_2$-$0.02CeO_2$ mixed oxide catalyst were also obtained by the EDX analysis, as shown in Figure 4.8. The elemental area mappings show that the Ti and Ce species were well dispersed throughout the bulk mesoporous-assembled $0.98TiO_2$-$0.02CeO_2$ mixed oxide catalyst. In order to obtain the information about the particle size of the mesoporous-assembled TiO_2-CeO_2 mixed oxide catalysts, the TEM analysis was performed. Figure 4.9 exemplifies the TEM image of the mesoporous-assembled $0.98TiO_2$-$0.02CeO_2$ mixed oxide catalyst

calcined at 500 °C with its corresponding EDX point mapping. The presence of both the Ti and Ce species was confirmed. The average particle size of the mixed oxide catalyst was in the range of 5-10 nm, which agrees well with its crystallite size estimated from the XRD analysis (Table 4.5).

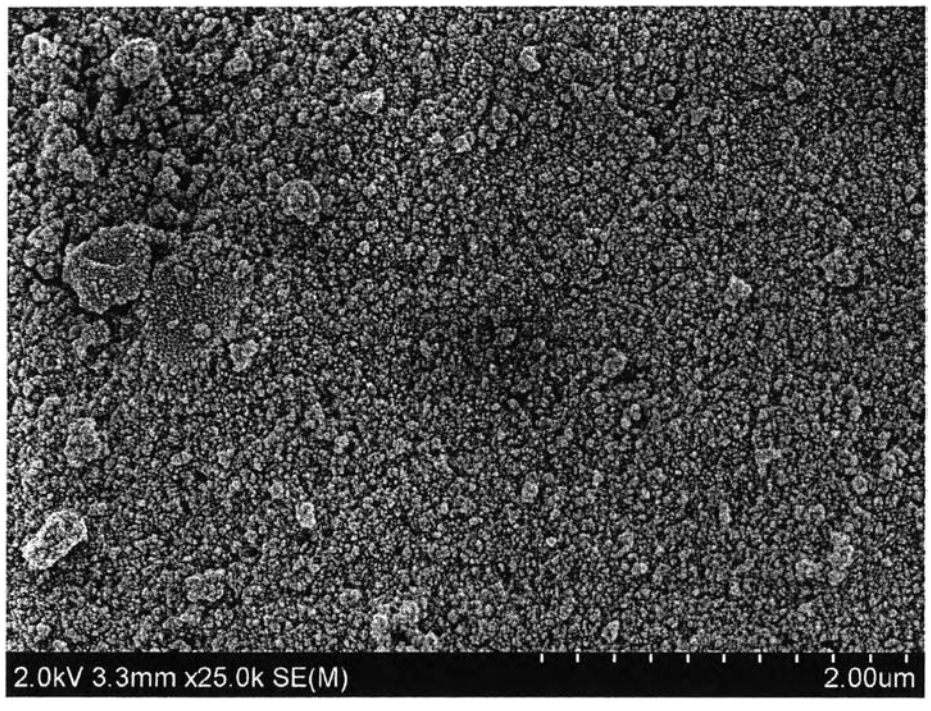

Figure 4.7 SEM image of the synthesized mesoporous-assembled $0.98TiO_2$-$0.02CeO_2$ mixed oxide catalyst calcined at 500 °C.

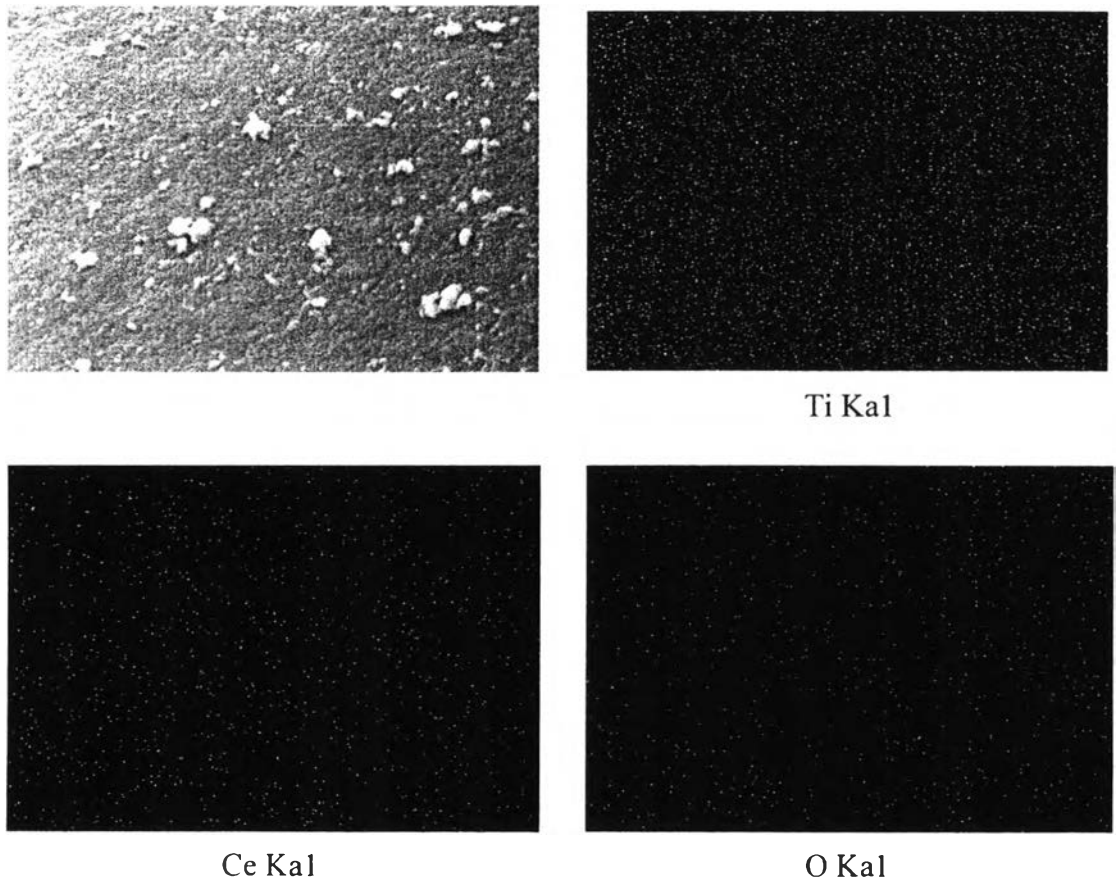

Figure 4.8 SEM image and EDX area mappings of the synthesized mesoporous-assembled $0.98TiO_2$-$0.02CeO_2$ mixed oxide catalyst calcined at 500 °C.

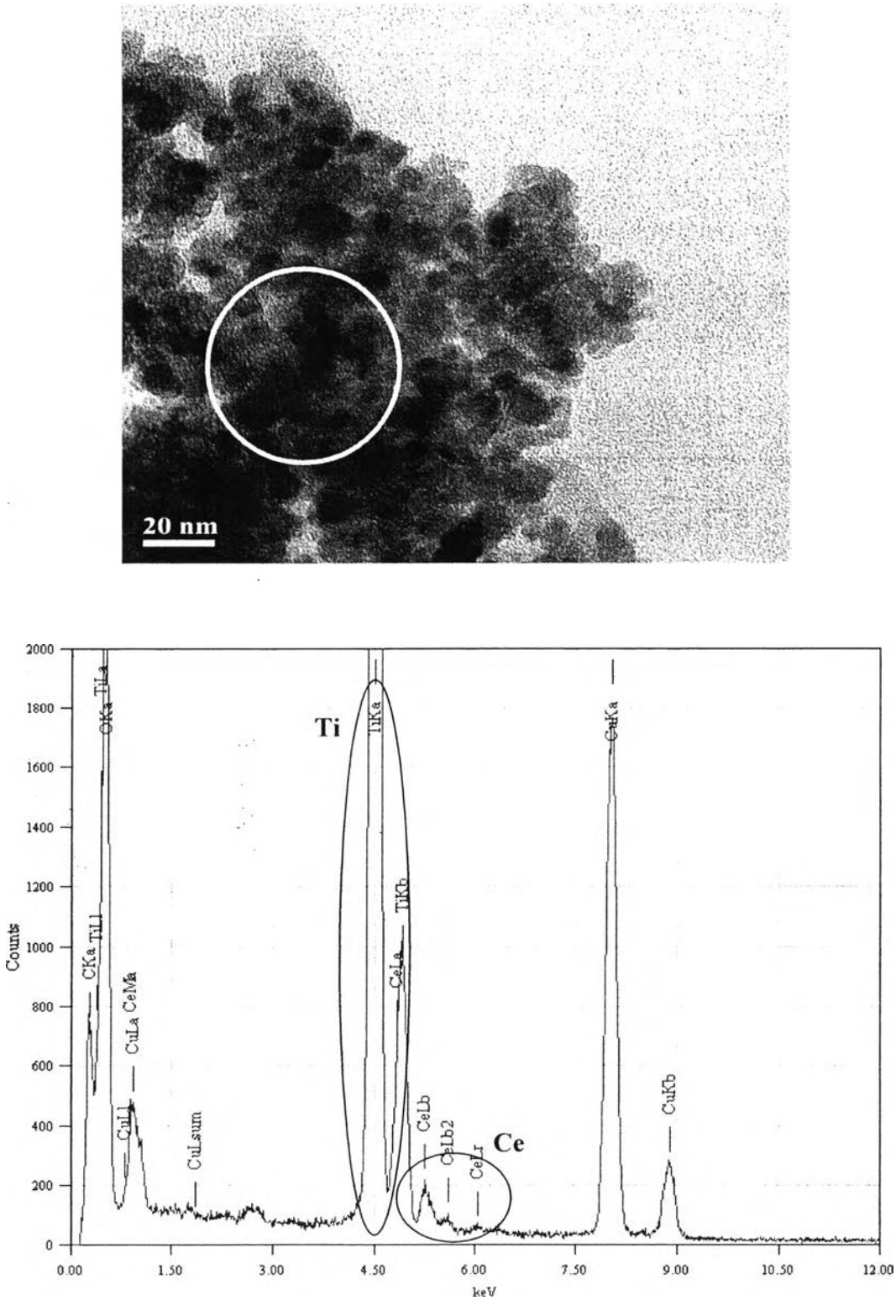

Figure 4.9 TEM image and EDX point mapping of the synthesized mesoporous-assembled $0.98TiO_2$-$0.02CeO_2$ mixed oxide catalyst calcined at 500°C.

4.3 Catalytic Activity Results of Cyclohexene Epoxidation

4.3.1 Blank Test

Cyclohexene epoxidation reaction was initially studied with control experiments in order to determine the effects of catalyst (synthesized mesoporous-assembled $0.98TiO_2$-$0.02CeO_2$ mixed oxide, which exhibited the highest epoxidation performance, as shown in next section) and oxidant (H_2O_2). The control experiments were performed under 3 different conditions, including case 1: without catalyst (with oxidant), case 2: without oxidant (with catalyst), and case 3: without both catalyst and oxidant. The results of cyclohexene conversion and product selectivities for all the cases are shown in Table 4.6. It was found that the reaction did not occur in the case without both the catalyst and oxidant. On the other hand, the reaction only slightly occurred in the case without catalyst and scarcely occurred in the case without oxidation, with the case without catalyst exhibiting a higher conversion (1.67 %) than that without oxidant (only 0.25 %). For the case of without catalyst (with oxidant), the results show the auto-oxidation of cyclohexene to form cyclohexene oxide and 2-cyclohexen-1-ol with very low selectivity, as well as 2-cyclohexen-1-one with comparatively much higher selectivity. This is possibly due to the strong oxidizing ability of H_2O_2, where it reacts with *tert*-butanol to primarily form the in situ generated *tert*-butyl hydroperoxide (t-BuOOH), which functions as a major source of the initiator to generate active free radicals upon thermal decomposition, such as *tert*-butoxy radical (t-BuO$^{\bullet}$) and hydroxyl radical (OH$^{\bullet}$) (Sreethawong *et al.*, 2005), as shown in Figure 4.10. These free radicals can react with cyclohexene to form cyclohexene radical, which further reacts with molecular O_2 to form intermediate cyclohexene peroxide radical. Since such intermediate peroxide radical has low thermal stability, it further decomposes to form non-radical primary products, which are cyclohexene oxide (epoxide) and 2-cyclohexen-1-ol (alcohol). Due to the presence of the mentioned active free radicals, these primary products further transform via free radical oxidation to finally form 2-cyclohexen-1-one (ketone), as observed in Table 4.6. The similar results were also observed for the case of without oxidant (with catalyst). This implies that with the aid of the hydroxyl groups on the catalyst surface, the *tert*-butanol may also be thermally decomposed to form free radicals that are

initiators for the aforementioned chain reactions, but with less probability, resulting in the observed lower conversion as compared to the case without catalyst (with oxidant). The overall results indicate that both the catalyst and oxidant are required for the cyclohexene epoxidation reaction.

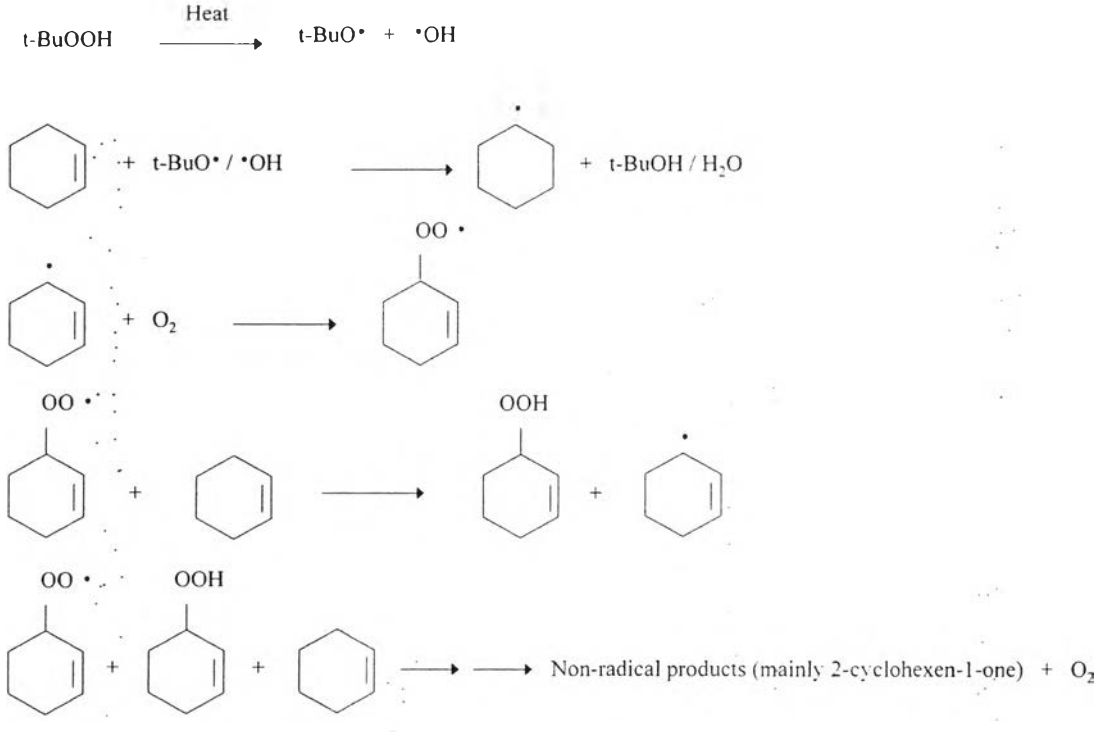

Figure 4.10 Proposed pathway for cyclohexene auto-oxidation.

Table 4.6 Control experiments for cyclohexene epoxidation by (1) without catalyst, (2) without oxidant, and (3) without both catalyst and oxidant (Reaction conditions: cyclohexene 30 mmol; *tert*-butanol 30 ml; H_2O_2 30 mmol; the synthesized mesoporous-assembled $0.98TiO_2$-$0.02CeO_2$ mixed oxide catalyst; reaction temperature 70 °C; reaction time 5 h)

		Case 1: No catalyst	**Case 2: No H_2O_2**	**Case 3: No catalyst and H_2O_2**
Cyclohexene conversion (%)		1.67	0.25	0
Selectivity (%)	Cyclohexene oxide	4.40	3.61	0
	2-Cyclohexen-1-ol	8.76	6.01	0
	2-Cyclohexen-1-one	86.85	90.38	0
	(1S,2S)-*trans*-1,2-cyclohexanediol	0	0	0

4.3.2 Effect of TiO_2-to-CeO_2 Molar Ratio in Mixed Oxide Catalysts

The synthesized mesoporous-assembled TiO_2-CeO_2 mixed oxide catalysts with various TiO_2-to-CeO_2 molar ratios were tested for the cyclohexene epoxidation with H_2O_2. The catalytic performances of the catalysts in terms of cyclohexene conversion and product selectivities as a function of TiO_2-to-CeO_2 molar ratio in terms of CeO_2 content are shown in Figure 4.11. It can be seen that even though the slight change in the cyclohexene conversion over the catalysts was observed, the $0.98TiO_2$-$0.02CeO_2$ mixed oxide catalyst (with 2 mol% CeO_2) provided the highest cyclohexene oxide selectivity (desired product) and comparatively low undesired product selectivities. According to the specific surface area analysis (Table 4.4), the incorporation of CeO_2 to TiO_2 increased the specific surface area of the catalyst, which basically resulted in more active sites on the catalyst surface; however, too much CeO_2 incorporation (higher than 2 mol%) caused a decrease in the cyclohexene oxide selectivity, indicating that the specific surface area is not a prime factor governing the cyclohexene epoxidation. Based on the proposed pathway for cyclohexene epoxidation at TiO_2 surface (see Figure 2.7), where the cyclohexene epoxidation was performed in *tert*-butanol-H_2O_2 system, *tert*-butyl hydroperoxide (t-

BuOOH) was generated at the early stage. Upon the exposure of the hydroxyl group on the TiO_2 surface (Ti-OH) with *tert*-butyl hydroperoxide, the *tert*-butyl peroxotitanium complex was formed. The cyclohexene epoxidation was then proceeded by oxygen transfer from the *tert*-butyl peroxotitanium complex to the cyclohexene double bond to form cyclohexene oxide (Sreethawong *et al.*, 2005). This proposed pathway points out that the surface OH group significantly affects the cyclohexene epoxidation activity in the way that the higher number of surface OH groups can induce more cyclohexene oxide formation. As clearly observed from Table 4.3, both the surface OH density and surface OH-to-catalyst weight ratio reached maximum values at the CeO_2 content of 2 mol%, which agree well with the observed maximum cyclohexene oxide selectivity. The results confirm that the synthesized mesoporous-assembled $0.98TiO_2$-$0.02CeO_2$ mixed oxide catalyst possessing the largest number of surface OH groups was the most suitable for the cyclohexene epoxidation in this work. Moreover, this catalyst exhibited a much higher cyclohexene oxide selectivity (44.37 %) as compared to the commercially available non-mesoporous-assembled P-25 TiO_2 (27.46 % with the cyclohexene conversion of 13 % under the identical reaction conditions).

(a)

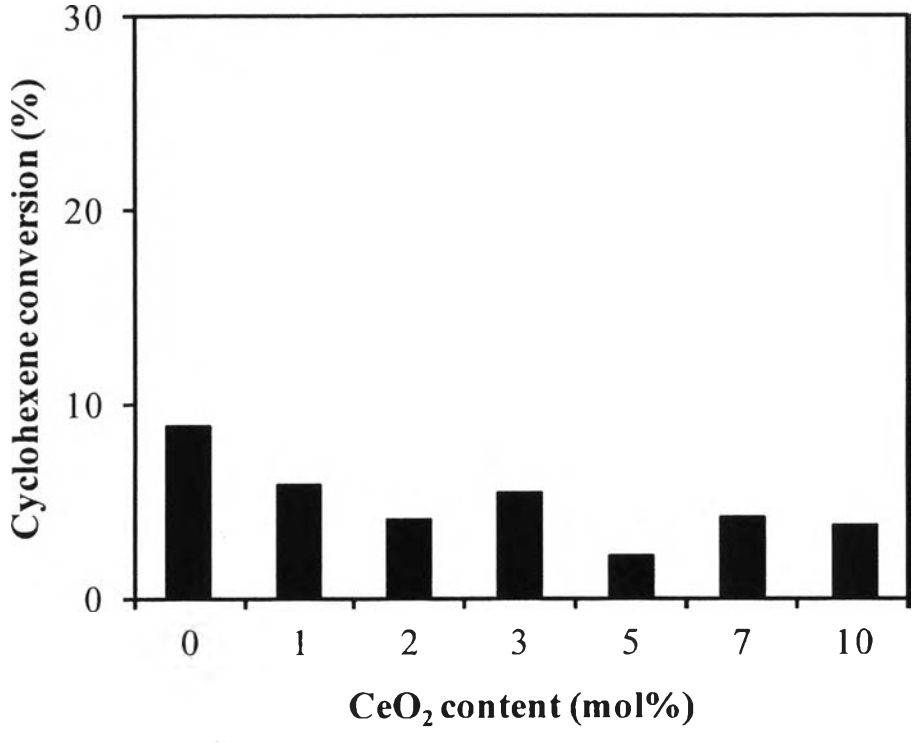

(b)

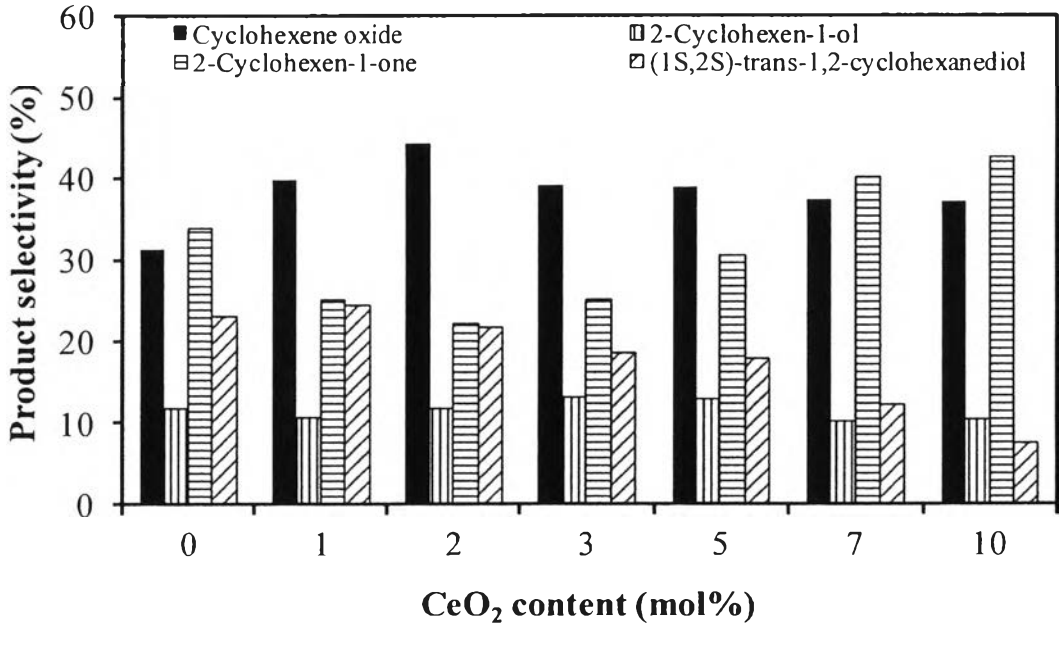

Figure 4.11 Effect of TiO_2-to-CeO_2 molar ratio in terms of CeO_2 content on (a) cyclohexene conversion and (b) product selectivities over the synthesized mesoporous-assembled TiO_2-CeO_2 mixed oxide catalysts calcined at 500 °C (Reaction conditions: cyclohexene 30 mmol; *tert*-butanol 30 ml; H_2O_2 30 mmol; reaction temperature 70 °C; reaction time 5 h).

4.3.3 Effect of H_2O_2-to-Cyclohexene Molar Ratio

The H_2O_2 concentration is another significant parameter affecting the cyclohexene oxide selectivity to be further optimized. By maintaining the cyclohexene amount constant, the effect of H_2O_2 concentration was studied over a wide range of H_2O_2-to-cyclohexene molar ratio from 0.125:1 to 2:1 using the synthesized mesoporous-assembled $0.98TiO_2$-$0.02CeO_2$ mixed oxide catalyst calcined at 500 °C. The effect of H_2O_2-to-cyclohexene molar ratio on the cyclohexene conversion and product selectivities is shown in Figure 4.12. It was observed that the increase in the H_2O_2-to-cyclohexene molar ratio enhanced the cyclohexene conversion, but not significantly, whereas the cyclohexene oxide selectivity increased with increasing H_2O_2-to-cyclohexene molar ratio until reaching a maximum at 0.25:1 and then decreased with further increasing H_2O_2-to-cyclohexene molar ratio. At the H_2O_2-to-cyclohexene molar ratio higher than 0.25:1, large amount of H_2O_2 might be left in the solution phase, being able to react with cyclohexene via free radical chain reactions upon the aforementioned auto-oxidation pathway. In conjunction with the surface epoxidation reaction pathway, these eventually resulted in higher undesired product selectivities and lower cyclohexene oxide selectivity. On the other hand, at the H_2O_2-to-cyclohexene ratio lower than 0.25:1, the oxygen transfer reaction at the catalyst surface to form cyclohexene oxide as the main product might less predominantly occur, due to the limited quantity of H_2O_2 available to form *tert*-butyl peroxotitanium complex for the cyclohexene epoxidation. Therefore, a well-controlled balance of the H_2O_2-to-cyclohexene molar ratio is required in order to achieve high cyclohexene oxide selectivity and low undesired product selectivities, exhibiting the optimum H_2O_2-to-cyclohexene molar ratio of 0.25:1 in this work. Moreover, when comparing the obtained optimum H_2O_2-to-cyclohexene molar ratio with the optimum ratio of 1:1 in a previous work using the RuO_2-loaded mesoporous-assembled TiO_2 catalyst prepared by incipient wetness impregnation method and calcined at 550 °C (Woragamon, 2009), it was found that regardless of other optimum reaction conditions, a lower H_2O_2 amount was required in this work using the mesoporous-assembled $0.98TiO_2$-$0.02CeO_2$ mixed oxide catalyst, which possessed a higher surface OH-to-catalyst weight ratio (6.83×10^{20} OH/g) than that of the catalyst used in the previous work (3.92×10^{20} OH/g).

(a)

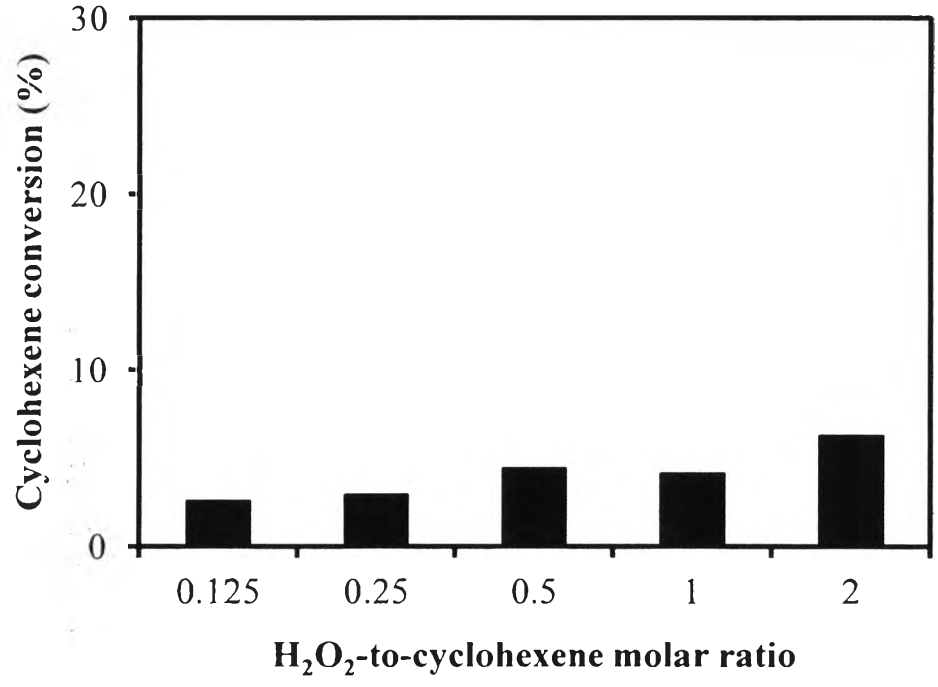

(b)

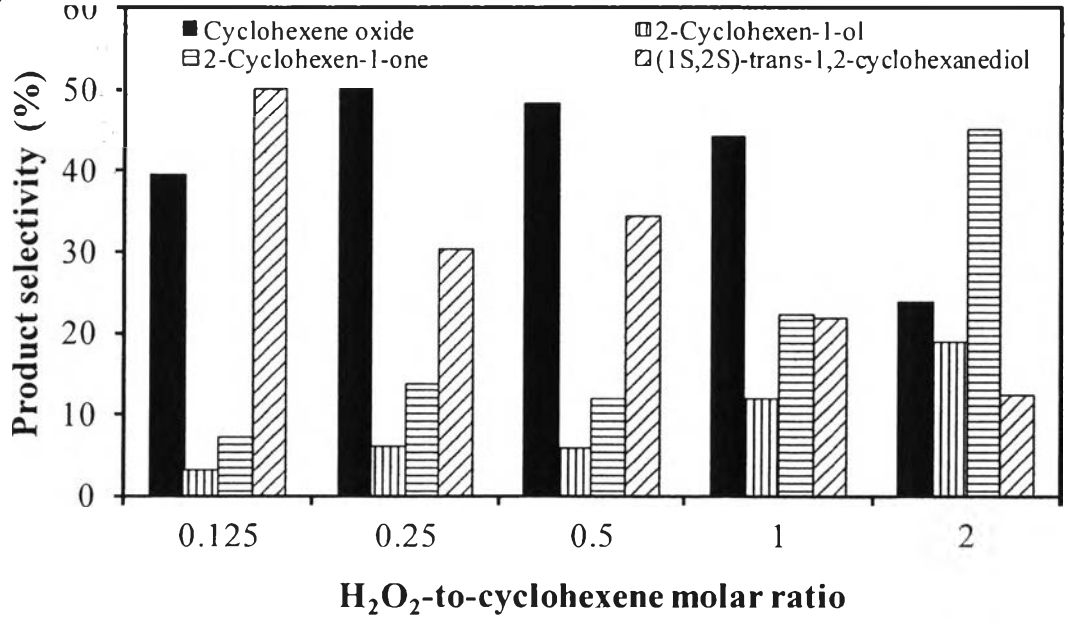

Figure 4.12 Effect of H_2O_2-to-cyclohexene molar ratio on (a) cyclohexene conversion and (b) product selectivities over the synthesized mesoporous-assembled $0.98TiO_2$-$0.02CeO_2$ mixed oxide catalyst calcined at 500 °C (Reaction conditions: cyclohexene 30 mmol; *tert*-butanol 30 ml; catalyst 0.5 g; reaction temperature 70 °C; reaction time 5 h).

4.3.4 Effect of Calcination Temperature

The effect of calcination temperature of the synthesized mesoporous-assembled $0.98TiO_2$-$0.02CeO_2$ mixed oxide catalyst was further investigated for the cyclohexene epoxidation by using the H_2O_2-to-cyclohexene molar ratio of 0.25:1. The results of cyclohexene conversion and product selectivities at different calcination temperatures in the range of 450 to 600 °C are shown in Figure 4.13. It could be seen that the cyclohexene conversion only slightly increased with increasing calcination temperature, whereas distinct differences in the product selectivities were observed. The calcination temperature of 500 °C provided a higher cyclohexene oxide selectivity with lower product selectivities as compared to the other calcination temperatures. Even though the calcination temperature of 450 °C resulted in the $0.98TiO_2$-$0.02CeO_2$ mixed oxide catalyst with a higher specific surface area as compared to 500 °C (Table 4.4), the less degree of crystallization at the lower calcination temperature of 450 °C (Figure 4.6) negatively resulted in a lower quantity of surface OH groups (Table 4.3), leading to less probability of the epoxidation reaction pathway at the catalyst surface. Moreover, when further increasing calcination temperature higher than 500 °C, the decrease in surface OH groups due to the specific surface area reduction (Table 4.4) and the crystal growth (Table 4.5) unfavorably decreased the cyclohexene oxide selectivity. Therefore, the calcination temperature of the catalyst was required to be suitably controlled in order to achieve the most active catalyst surface possessing the largest quantity of OH groups. It can be concluded that the optimum calcination temperature of the synthesized mesoporous-assembled $0.98TiO_2$-$0.02CeO_2$ mixed oxide catalyst in this work was 500 °C, providing the highest cyclohexene oxide selectivity.

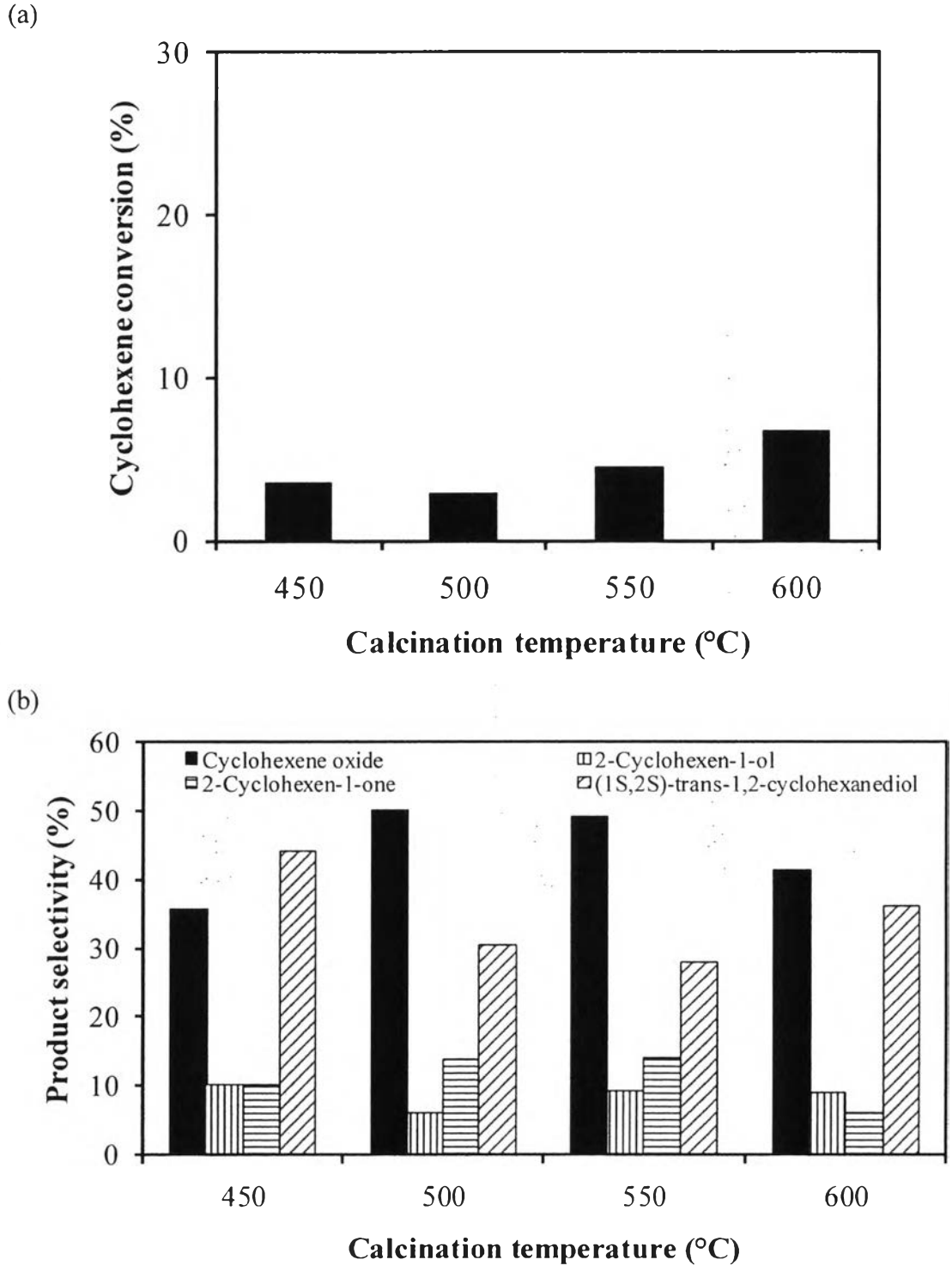

Figure 4.13 Effect of calcination temperature of the synthesized mesoporous-assembled $0.98TiO_2$-$0.02CeO_2$ mixed oxide catalyst on (a) cyclohexene conversion and (b) product selectivities (Reaction conditions: cyclohexene 30 mmol; *tert*-butanol 30 ml; H_2O_2 7.5 mmol; catalyst 0.5 g; reaction temperature 70 °C; reaction time 5 h).

4.3.5 Effect of Catalyst-to-Reaction Volume Ratio

The effect of the content of the synthesized mesoporous-assembled $0.98TiO_2$-$0.02CeO_2$ mixed oxide catalyst in terms of catalyst-to-reaction volume ratio on the cyclohexene epoxidation activity was further examined. The results of cyclohexene conversion and product selectivities as a function of catalyst-to-reaction volume ratio are shown in Figure 4.14. Regardless of the almost unchanged cyclohexene conversion with respect to the catalyst-to-rection volume ratio, it could be seen that the cyclohexene oxide selectivity increased with increasing catalyst-to-reaction volume ratio from 1.67 mg/ml to reach a maximum value at 3.33 mg/ml and then decreased with further increasing catalyst-to-reaction volume ratio. The initial increase in the catalyst-to-reaction volume ratio simply increases the surface active sites available for the surface epoxidation reaction, as expected. However, when the catalyst-to-reaction volume ratio exceeded a critical limit of 3.33 mg/ml, the aggregation among the catalyst particles during the reaction might be more dominant, resulting in a loss of reactant accessibility to the available surface active sites and subsequently lowering the overall catalytic activity. The results suggest that an excess catalyst amount is not required for the cyclohexene epoxidation via the surface oxygen transfer pathway, of which the largest accessible surface OH groups are essentially important. Therefore, the optimum catalyst-to-reaction volume ratio in this work was considered to be 3.33 mg/ml. In addition, such optimum catalyst-to-reaction volume was relatively lower than the optimum value of 16.67 mg/ml obtained in the previous work (Woragamon, 2009). This indicates that under any operating conditions with different catalyst types, the catalyst amount required to obtain the highest cyclohexene oxide selectivity must be optimized.

(a)

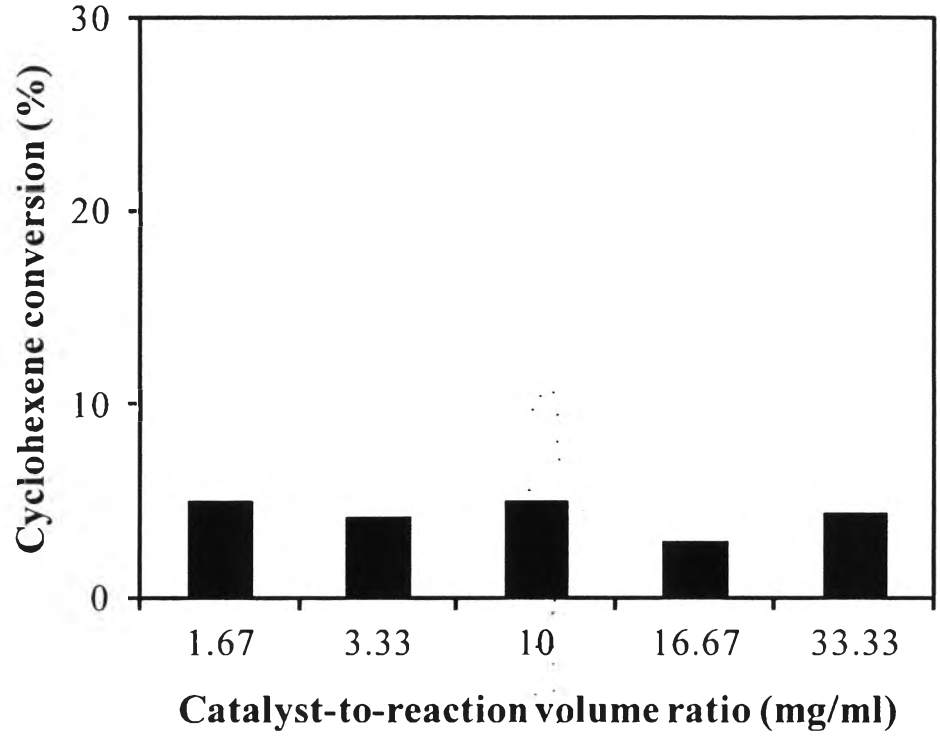

(b)

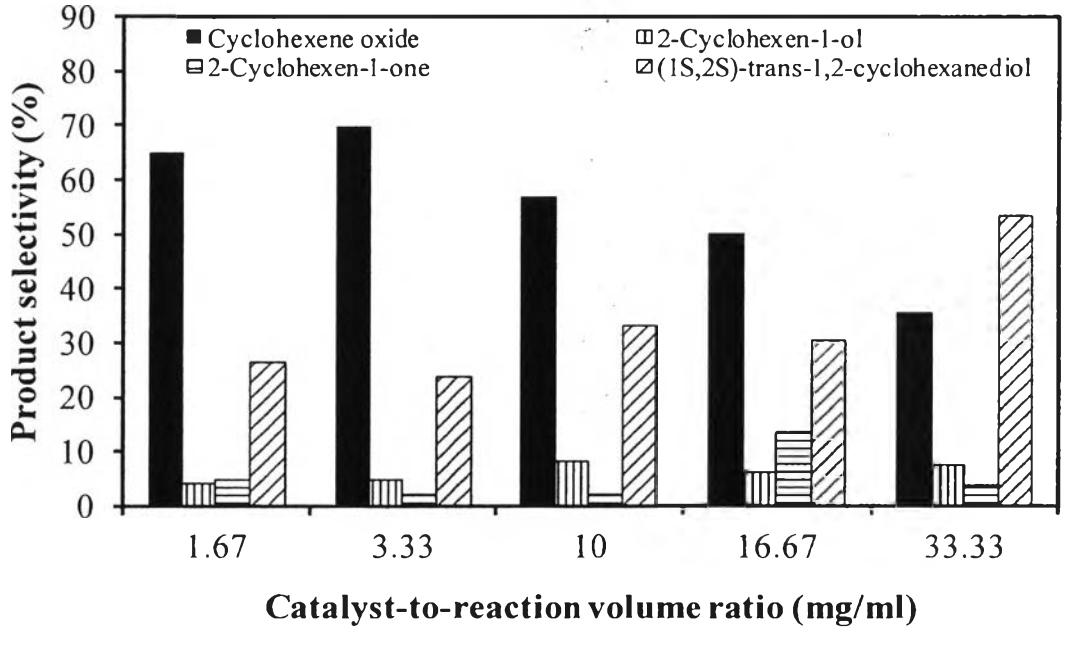

Figure 4.14 Effect of catalyst-to-reaction volume ratio on (a) cyclohexene conversion and (b) product selectivities over the synthesized mesoporous-assembled $0.98TiO_2$-$0.02CeO_2$ mixed oxide catalyst calcined at 500 °C (Reaction conditions: cyclohexene 30 mmol; *tert*-butanol 30 ml; H_2O_2 7.5 mmol; reaction temperature 70 °C; reaction time 5 h).